Studying the Lipkin model using the VQE algorithm.

FYS-5429

Written by:

Odin Johansen

Department of Physics UiO

UiO : University of Oslo

April 2, 2024

Contents

1. Abstract

In the realm of quantum mechanics, efficiently computing the energy levels indicated by the eigenvalues of a system's Hamiltonian is essential, especially for complex systems requiring the identification of the ground state. The Variational Quantum Eigensolver (VQE), a numerical approach in quantum computing, offers a promising solution by utilizing the variational principle to estimate the ground state energy. This hybrid quantum-classical method optimally combines quantum state preparation and measurement with classical optimization.
Applied to both simple 2x2 and more complex four-particle Hamiltonians, VQE demonstrates its efficacy by accurately approximating analytical solutions across various interaction strengths. Notably, for the Lipkin-Meshkov-Glick model, VQE surpasses traditional approximation methods, such as Hartree-Fock, particularly in systems of up to four qubits. The performance of VQE highlights the crucial role of the ansatz choice in achieving accurate results, even in the presence of off-diagonal Hamiltonian elements that introduce significant complexity. In essence, VQE's ability to reproduce and outperform classical computational methods in finding the lowest energy eigenvalue of Hamiltonians showcases its potential as a powerful tool in quantum computing, promising advancements in the simulation of quantum systems.

2. Introduction

The Lipkin model, a simplified representation of many-body systems in nuclear physics, serves as the focus of this study within the context of quantum computing and quantum machine learning. This project aims to analyze the model using the Variational Quantum Eigensolver (VQE) algorithm, a hybrid quantum-classical approach tailored for noisy intermediate-scale quantum (NISQ) computers. By leveraging the computational capabilities of both classical and quantum processors, VQE offers a promising pathway for solving the eigenvalue problem associated with the Lipkin Hamiltonian.
Our analysis begins with the implementation of basic quantum operations, including the application of Pauli matrices and the generation of entangled states via Bell states. This foundational work supports the subsequent exploration of the Lipkin model, where we employ VQE to approximate the ground state energy of a simplified Hamiltonian system. Through a systematic approach, we investigate the effects of varying interaction strengths on the system's energy levels and entanglement properties.
In this context, the project not only explores the application of quantum algorithms to a well-defined physical model but also compares the outcomes of quantum simulations with classical eigenvalue solution methods. By doing so, we aim to quantify the efficacy of VQE in addressing quantum mechanical problems and to identify potential advantages and limitations of quantum computational approaches in simulating complex quantum systems.
This study contributes to the ongoing development of quantum algorithms for quantum simulation, providing insights into the operational principles of the VQE algorithm and its applicability to the study of quantum many-body systems through the lens of the Lipkin model.

3. Theory

i. Quantum Mechanics and Computational Notation

Qubits and Classical Bits At the heart of Quantum Computing (QC) lies the qubit, a unit analogous to the binary digit in Classical Computing (CC). Unlike classical bits that exist in a definite state of 0 or 1, qubits are two-state quantum systems characterized by their ability to exist in multiple states simultaneously due to quantum superposition.

Pauli Basis States:

$$|0\rangle = \begin{pmatrix} 1 \\ 0 \end{pmatrix}, \quad |1\rangle = \begin{pmatrix} 0 \\ 1 \end{pmatrix}. \tag{1}$$

These basis states form the foundation for representing qubits in quantum mechanics.

Superposition and Normalization: A qubit's state, $|\psi\rangle$, can be a superposition of its basis states, expressed as $|\psi\rangle = c_0|0\rangle + c_1|1\rangle$, where c_0 and c_1 are complex coefficients adhering to the normalization condition $|c_0|^2 + |c_1|^2 = 1$. This condition ensures the probabilities of measuring the qubit in either state sum to 1, reflecting the probabilistic nature of quantum measurements.

Quantum Entanglement: A phenomenon where qubits become interconnected, allowing the state of one qubit to instantaneously affect another regardless of distance. The Bell state, $|\Phi^+\rangle = \frac{1}{\sqrt{2}}(|00\rangle + |11\rangle)$, exemplifies maximal entanglement between two qubits.

Quantum Gates and Operations: Quantum gates, the operational elements of QC, manipulate qubits through unitary matrices. These gates include the Pauli matrices (X, Y, Z) shown in equation (2), which represent fundamental quantum operations. Composite systems and multi-qubit operations utilize tensor products, enabling complex quantum algorithms that outperform classical counterparts for specific tasks.

$$X = \begin{pmatrix} 0 & 1 \\ 1 & 0 \end{pmatrix}, \quad Y = \begin{pmatrix} 0 & -i \\ i & 0 \end{pmatrix}, \quad Z = \begin{pmatrix} 1 & 0 \\ 0 & -1 \end{pmatrix} \tag{2}$$

A three-qubit operation, $X_1Y_3 = X \otimes I \otimes Y$, demonstrates the application of gates across multiple qubits, modifying their states in a controlled fashion.

ii. Introduction to Quantum Computing and Algorithms

Quantum computing promises to revolutionize our computational capabilities through principles fundamentally different from classical computing. This section focuses on the pivotal elements of quantum circuits and states, essential for understanding and utilizing the full potential of quantum computing. We will explore the architecture of quantum circuits, the roles of quantum states, and the critical operations that manipulate these states, using the Greenberger-Horne-Zeilinger (GHZ) state as a primary example of quantum entanglement in action.

Entanglement, a cornerstone of quantum computing, allows qubits to be connected in such a way that the state of one (no matter the distance) can depend on that of another. We illustrate this through the GHZ State, a configuration of three or more qubits that are fully entangled, and its simpler counterpart, the Bell state, involving just two qubits.

The construction of these entangled states is facilitated by quantum gates. The Hadamard gate, for example, puts a qubit into a superposition state, while the Controlled NOT (CNOT) gate entangles two qubits. The mathematical representations of these gates are as follows:

$$H_{\text{adamard}} = \frac{1}{\sqrt{2}} \begin{pmatrix} 1 & 1 \\ 1 & -1 \end{pmatrix}, \quad CNOT = \begin{pmatrix} 1 & 0 & 0 & 0 \\ 0 & 1 & 0 & 0 \\ 0 & 0 & 0 & 1 \\ 0 & 0 & 1 & 0 \end{pmatrix}, P = \begin{pmatrix} 1 & 0 \\ 0 & i \end{pmatrix}, \tag{3}$$

Understanding these gates and their operations provides the foundation for creating entangled states like the GHZ state.
Further enriching our quantum toolkit are rotation operators: Rx, Ry, and Rz. These operators allow for the precise manipulation of qubit states, enabling them to reach any point on the Bloch sphere, a representation of a qubit's state in three-dimensional space.

$$Rx(\theta) = e^{-iX\theta/2} = \begin{pmatrix} \cos(\theta/2) & -i\sin(\theta/2) \\ -i\sin(\theta/2) & \cos(\theta/2) \end{pmatrix}, \tag{4}$$

$$Ry(\theta) = e^{-iY\theta/2} = \begin{pmatrix} \cos(\theta/2) & -\sin(\theta/2) \\ \sin(\theta/2) & \cos(\theta/2) \end{pmatrix}, \tag{5}$$

$$Rz(\theta) = e^{-iZ\theta/2} = \begin{pmatrix} e^{-i\theta/2} & 0 \\ 0 & e^{i\theta/2} \end{pmatrix}. \tag{6}$$

These operations are crucial for the versatile manipulation of qubit states, underpinning many quantum computing algorithms and applications.

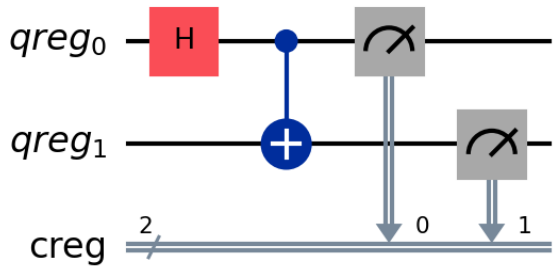

Figure 1. The Quantum Circuit used to initialize a Bell-state. This circuit consists of one Hadamard gate and one CNOT gate.

To make the circuit from figure(1) into a GHZ state, you only need to add another qubit and CNOT gate to entangle them. The result of this circuit is full entanglement, this can be made clear by the visualization in figure(2) of the bloch sphere. If one of the states is measured we know the state of the other.
This fact is displayed well in figure(3) if we measure it about 1000 times, to see that it should be about 50/50 for the two states.

Quantum Algorithms The emergence of quantum algorithms has unlocked new avenues for solving problems too time-consuming for classical computers. These algorithms use quantum states, entanglement, and superposition to perform computations. For example, Shor's algorithm has transformed the world of cryptography by enabling the

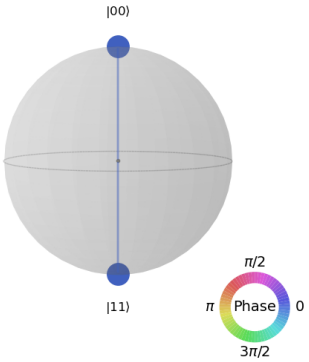

Figure 2. The Quantum Circuit used to initialize a Bell-state. This circuit consists of one Hadamard gate and one CNOT gate.

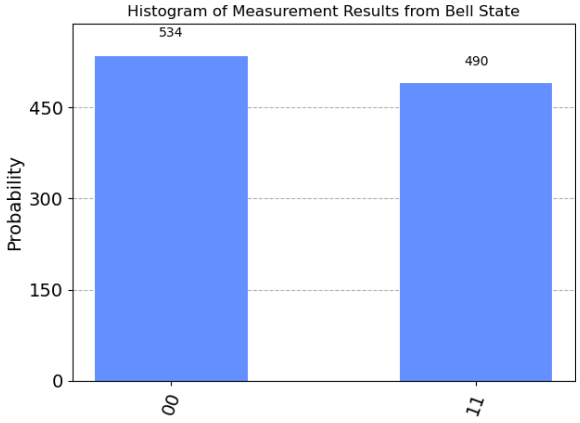

Figure 3. The Quantum Circuit used to initialize a Bell-state. This circuit consists of one Hadamard gate and one CNOT gate.

factoring of large integers in polynomial time, something classical algorithms have struggled to achieve. Similarly, Grover's algorithm provides a quadratic speedup for searching unsorted databases, demonstrating the potential of quantum computing to significantly reduce computational times for specific tasks.

Quantum algorithms are designed to exploit the unique capabilities of quantum systems. These features allow quantum computers to explore a vast computational space more efficiently than classical computers for certain problems. Developing and implementing quantum algorithms requires a deep understanding of quantum mechanics, as well as innovative approaches to algorithm design and optimization.

iii. Principles of the Variational Quantum Eigensolver

The Variational Quantum Eigensolver (VQE) is a crucial tool in quantum computing, particularly for solving eigenvalue problems associated with quantum systems. Its efficacy hinges on the precise representation of the system's Hamiltonian. This representation involves reformulating the Hamiltonian as a sum of Pauli strings, leveraging the foundational elements of quantum mechanics - the identity operator I and the Pauli matrices$X, Y,$

and Z. To construct a term within this framework, one utilizes the tensor product of these operators, denoted as P_i, across an n-qubit system. This necessitates n-1 tensor products to articulate a single term effectively. Each term is further characterized by a specific weight w_i, culminating in the Hamiltonian's representation as:

$$H = \sum_i w_i P_i \tag{7}$$

The process of transforming a general two-body Hamiltonian into this succinct form poses considerable challenges. However, transformation schemes like the Jordan-Wigner transformation offer systematic methodologies for such conversions. In particular, models such as the Lipkin model allow for a more straightforward adaptation, enabling the Hamiltonian to be directly delineated as products of number and spin operators, simplifying the overall complexity.

Introduction to the Variational method The Variational Method (VM) is highly effective in approximating the ground state energy of quantum systems governed by a Hamiltonian H. At the heart of this method lies the construction of an expectation value from a carefully chosen trial wave function, or ansatz $|A\rangle$, which inherently sets a lower boundary for the system's ground state energy E_0. This foundational concept is encapsulated by the inequality:

$$\frac{\langle A|H|A\rangle}{\langle A|A\rangle} \geq E_0 \tag{8}$$

In practical applications, the ansatz $|A\rangle$ is formulated as a parameterized superposition of basis states, symbolized as $|A\rangle \equiv |A(\theta)\rangle$. Here, the vector θ, consisting of M adjustable parameters $(\theta_1, \ldots, \theta_M)$, is meticulously optimized to refine the estimate of the energy minimum.
This variational technique proves indispensable in the study of many-body physics, where direct analytical solutions remain elusive for the ground state energies of complex systems. Unlike perturbation theory, which risks underestimating these energies, the Variational Method ensures that the chosen ansatz possesses some degree of overlap with the actual ground state, thereby mitigating such inaccuracies. It is this principle that forms the foundation of the Variational Quantum Eigensolver (VQE), enabling precise estimations of ground state energies in multifaceted quantum systems.

The Variational method Algorithm The goal is to leverage the Variational Method (VM) to approximate the ground state energy of a specified Hamiltonian. This entails the parametrization of the ansatz $|A\rangle$ to introduce adaptability in its construction. A widely adopted approach utilizes the Ry ansatz, characterized by sequential rotations around the y-axis on the Bloch sphere through angles $\theta = (\theta_1, \ldots, \theta_Q)$, interspersed with CNOT operations. The choice of y-axis rotations is pivotal, ensuring the state vector's coefficients remain real, a condition often sufficient for analyzing many-body systems.
Following the ansatz construction, the Hamiltonian expressed as a sum of Pauli strings is applied. The expectation value of the ground state energy can thus be computed through the aggregate expectation values of each component within the Pauli string set:

$$E(\theta) = \sum_i w_i \langle A(\theta)|P_i|A(\theta)\rangle \equiv \sum_i w_i f_i, \tag{9}$$

where f_i represents the expectation value for the i-th Pauli string. These expectation values are statistically deduced by measuring the outcome frequencies in the eigenbases corresponding to each operator in the Pauli string. For example, should P_i include Z_1, the analysis involves computing the net difference between the 0 and 1 outcomes for the first qubit, averaged over numerous measurements. If P_i encompasses X_2, then measurements for the second qubit align along the x-axis. Defining N_0 and N_1 as the counts of 0 and 1 outcomes respectively, f_i is estimated by:

$$f_i = \lim_{N\to\infty} \frac{N_0 - N_1}{N}, \tag{10}$$

where N signifies the total count of measurements or shots. Accordingly, each Pauli string mandates a unique circuit configuration for repeated measurements, collectively enabling an estimation of the ground state energy. The optimization of θ is typically facilitated by a classical optimizer, where gradients are approximated through the finite difference method:

$$\nabla_\theta E(\theta) \approx \frac{E(\theta + \delta\theta) - E(\theta - \delta\theta)}{2\delta\theta}, \tag{11}$$

with $\delta\theta = (\delta\theta_1, \ldots, \delta\theta_Q)$. The iterative refinement of θ parameters, driven by the negative gradient, yields a progressively optimized set of parameters. This iterative process persists until convergence upon the minimum energy state or an acceptably proximate approximation thereof is realized. The efficacy of this methodology critically hinges on the initial selection of an ansatz that affords significant versatility in state initialization, subsequently amendable through optimization to traverse towards more energetically favorable states.

iv. The Lipkin Model in Quantum Systems

When you are working with complex many-body systems, the occupation representation emerges as a fundamental framework. This representation facilitates the introduction of creation $a_p^\dagger$ and annihilation a_p operators, pivotal in defining the dynamics of fermionic systems. These operators adhere to canonical anti-commutation relations, indicative of the fermionic nature of the particles:

$$\{a_p^\dagger, a_q^\dagger\} = \{a_p, a_q\} = 0, \quad \{a_p^\dagger, a_q\} = \delta_{pq}. \tag{12}$$

The Lipkin model, pioneered by Lipkin [**?**], abstracts a system of N fermions into two energy levels $\sigma \in \{\pm 1\}$, each with a degeneracy of N. This model uniquely characterizes the system, with each level's occupancy altering the energy by $\pm\frac{1}{2}\epsilon$, thereby mirroring the essence of fermionic half-integer spins.
Employing creation and annihilation operators, the Lipkin Hamiltonian unfolds as:

$$H = H_0 + H_1 + H_2, \tag{13}$$

where H_0, H_1, and H_2 embody distinct operational mechanisms within the fermion system. Specifically,

$$H_0 = \frac{1}{2}\epsilon \sum_{pq\sigma} a_{p\sigma}^\dagger a_{p\sigma}, \tag{14}$$

representing a diagonal single-particle operator that calculates the energy contribution based on particle occupancy levels. Conversely, H_1 and H_2, expressed as

$$H_1 = \frac{1}{2}V \sum_{pp'\sigma} a_{p\sigma}^\dagger a_{p'\sigma}^\dagger a_{p'(-\sigma)} a_{p(-\sigma)}, \tag{15}$$

and

$$H_2 = \frac{1}{2}W \sum_{pp'\sigma} a_{p\sigma}^\dagger a_{p'(-\sigma)}^\dagger a_{p'\sigma} a_{p(-\sigma)}, \tag{16}$$

respectively, are two-body operators. These operators facilitate the movement and exchange of particle pairs between energy levels, encompassing both direct level transitions and spin-exchange interactions. The efficacy of these interactions is modulated by the coupling constants V and W, which parameterize the strengths of the respective effects within the fermion system.
In the analysis of fermion systems, the introduction of quasi-spin operators $J_\pm$, J_z, and J^2, alongside the number

operator N, provides a methodological advantage. These operators are defined as follows:

$$J_{\pm} = \sum_{p} a^{\dagger}_{p\pm} a_{p\mp}, \tag{17}$$

$$J_z = \frac{1}{2} \sum_{p\sigma} \sigma a^{\dagger}_{p\sigma} a_{p\sigma}, \tag{18}$$

$$J^2 = J_+ J_- + J_z^2 - J_z, \tag{19}$$

$$N = \sum_{p\sigma} a^{\dagger}_{p\sigma} a_{p\sigma}. \tag{20}$$

Utilizing these operators, the Lipkin Hamiltonian, previously articulated in equation(13), undergoes a significant transformation:

$$H_0 = \epsilon J_z, \tag{21}$$

$$H_1 = \frac{1}{2} V (J_+^2 + J_-^2), \tag{22}$$

$$H_2 = \frac{1}{2} W (\{J_+, J_-\} - N). \tag{23}$$

The quasi-spin operators adhere to the conventional spin commutator relations:

$$[J_z, J_{\pm}] = \pm J_{\pm}, \tag{24}$$

$$[J_+, J_-] = 2J_z, \tag{25}$$

$$[J^2, J_{\pm}] = 0, \tag{26}$$

$$[J^2, J_z] = 0, \tag{27}$$

they also commute with the number operator:

$$[N, J_z] = [N, J_{\pm}] = [N, J^2] = 0. \tag{28}$$

These commutator relations demonstrate that the Hamiltonian, a composite of quasi-spin operators and the number operator, shares an eigenbasis with J^2, thereby establishing J as a viable quantum number. Employing spin-eigenstates as the Hamiltonian basis, states are designated through $|J, J_z\rangle$, with J and J_z representing spin and spin-projections, respectively. The states at $J_z = \pm J$, indicating a level's complete occupancy, are straightforward to construct. Intermediate states are attainable via the quasi-spin ladder operators, adhering to:

$$J_{\pm}|J, J_z\rangle = \sqrt{J(J+1) - J_z(J_z \pm 1)}|J, J_z \pm 1\rangle. \tag{29}$$

From this the matrix elements of the quasi-spin Hamiltonian, denoted $H_{J_z, J_z'} = \langle J, J_z|H|J, J_z'\rangle$, can be made. For a system comprising $N = 2$ particles, we encounter a triplet configuration where $J = 1$, manifesting in three possible projection states $J_z = 0, \pm 1$. We know from analytical calculations that the Hamiltonian within the J basis assumes the form:

$$H = \begin{pmatrix} -\epsilon & 0 & V \\ 0 & W & 0 \\ V & 0 & \epsilon \end{pmatrix}. \tag{30}$$

Addressing the eigenvalue problem facilitates the precise determination of the ground state energy for this configuration.

Expanding the system to $N = 4$ particles results in $J = 2$, yielding five potential projection states $J_z = 0, \pm 1, \pm 2$. Applying the methodology the Hamiltonian is represented as:

$$H = \begin{pmatrix} -2\epsilon & 0 & \sqrt{6}V & 0 & 0 \\ 0 & -\epsilon + 3W & 0 & 3V & 0 \\ \sqrt{6}V & 0 & 4W & 0 & \sqrt{6}V \\ 0 & 3V & 0 & \epsilon + 3W & 0 \\ 0 & 0 & \sqrt{6}V & 0 & 2\epsilon \end{pmatrix}. \tag{31}$$

Benchmarking the VQE results for the Lipkin Model is done by comparing it with the solutions derived from the Hartree-Fock (HF) method and the Random Phase Approximation (RPA). The Lipkin Model permits exact solutions for these methods as well. The known Hartree-Fock solution[1] is expressed as:

$$E_{HF} = -\frac{N}{2}\begin{cases} \epsilon + W & \text{for } R < \epsilon, \\ \frac{\epsilon^2+(N-1)^2(V+W)^2}{2(N-1)(V+W)} + W & \text{for } R > \epsilon, \end{cases} \tag{32}$$

where $R \equiv (N-1)(V+W)$. The RPA solution, as reported by [1], is given by:

$$E_{\text{RPA}} = E_{\text{HF}} + \frac{\omega - A}{2}, \tag{33}$$

where $\omega = \sqrt{A^2 - |B|}$, and the coefficients A and B are specific to the considered region:

$$A = \begin{cases} \epsilon - (N-1)W & R < \epsilon \\ \frac{3(N-1)^2(V+W)^2-\epsilon^2}{2(N-1)(V+W)} - (N-1)W & R > \epsilon \end{cases}, \tag{34}$$

$$B = \begin{cases} -(N-1)V & R < \epsilon \\ -\frac{\epsilon^2+(N-1)^2(V+W)^2}{2(N-1)(V+W)} + (N-1)W & R > \epsilon \end{cases}. \tag{35}$$

4. Detailed System Analysis

This section will introduce the three different systems we are analyzing in this paper. Firstly we will look at two test models, a 2x2 and a 4x4 real Hamiltonian, each having arbitrary entries. The final model we are analyzing is called the Lipkin model, the reason for choosing this model is that while it is analytically solvable it showcases many essential properties of many-body systems.

i. 2x2 real Hamiltonian

In our preliminary investigation, we focus on a 2×2 real Hamiltonian, which is comprised of two distinct components: a diagonal component, H_0, and an off-diagonal component, H_I. These components symbolize the non-interacting one-body sector and the interacting two-body sector, respectively. Within the framework of the Pauli basis, defined as $\{|0\rangle, |1\rangle\}$, the Hamiltonian is formulated as follows:

$$H = H_0 + H_I, \tag{36}$$

where the diagonal part, H_0, represents the system's intrinsic energy levels without interaction and is given by:

$$H_0 = \begin{pmatrix} E_1 & 0 \\ 0 & E_2 \end{pmatrix}, \tag{37}$$

and the off-diagonal part, H_I, introduces the interaction between these levels, modulated by a coupling constant λ, as:

$$H_I = \lambda \begin{pmatrix} V_{11} & V_{12} \\ V_{21} & V_{22} \end{pmatrix}, \tag{38}$$

with the coupling constant λ ranging within the interval $[0, 1]$, thus parametrizing the interaction's intensity between the system's constituents.

ii. 4x4 real Hamiltonian

This section delves into a complex system represented by a 4×4 real Hamiltonian matrix, essentially viewed as two linked two-level systems. Employing the basis $\{|00\rangle, |01\rangle, |10\rangle, |11\rangle\}$, we first describe the system's non-interactive component with:

$$H_0 |ij\rangle = \epsilon_{ij} |ij\rangle, \tag{39}$$

where ϵ_{ij} are the energy levels. For the interactive part, we use Pauli matrices to account for two-body interactions, which is given by:

$$H_I = H_x \sigma_x \otimes \sigma_x + H_z \sigma_z \otimes \sigma_z, \tag{40}$$

This leads to the full Hamiltonian being:

$$H = \begin{pmatrix} \epsilon_{00} + H_z & 0 & 0 & H_x \\ 0 & \epsilon_{10} - H_z & H_x & 0 \\ 0 & H_x & \epsilon_{01} - H_z & 0 \\ H_x & 0 & 0 & \epsilon_{11} + H_z \end{pmatrix}, \tag{41}$$

Here, H_x and H_z are coupling constants, similar in role to λ in simpler setups, adjusting the interaction strengths within the system.

iii. Encodings

The Simple Systems

To start, we need to break down the Hamiltonian from equation (36) using Pauli matrices. Focusing on H_0 first, we fill its diagonal with different energy levels. We define the average and difference of these energies as:

$$E_+ = \frac{E_1 + E_2}{2}, \quad E_- = \frac{E_1 - E_2}{2}, \tag{42}$$

This step shows that a simple combination of the identity matrix and the Z Pauli matrix can neatly express H_0:

$$H_0 = E_+ I + E_- Z. \tag{43}$$

For H_1, we use a similar approach for the diagonal entries, introducing:

$$V_+ = \frac{V_{11} + V_{22}}{2}, \quad V_- = \frac{V_{11} - V_{22}}{2}. \tag{44}$$

Considering H is hermitian, and knowing $V_{12} = V_{21} \equiv V_o$, we simplify the expression to:

$$H_1 = V_+ I + V_- Z + V_o X. \tag{45}$$

When we move to discussing a 4×4 system, we see that the interactive part of Hamiltonian from equation(39) is already in terms of Pauli matrices, so we don't need to adjust it much. But, we do need to look again at the diagonal parts. Following a similar strategy to the 2×2 case, we define:

$$\epsilon_{\pm 0} = \frac{\epsilon_{00} \pm \epsilon_{01}}{2}, \quad \epsilon_{\pm 1} = \frac{\epsilon_{10} \pm \epsilon_{11}}{2}. \tag{46}$$

This approach allows us to represent the energies ϵ_{00} and ϵ_{01}, as well as ϵ_{10} and ϵ_{11}, uniformly across the diagonal, leading to:

$$D_0 = \epsilon_{+0} I \otimes I + \epsilon_{-0} I \otimes Z, \text{ and } D_1 = \epsilon_{+0} I \otimes I + \epsilon_{-1} I \otimes Z. \tag{47}$$

We can think of single qubit projector operators, using I and Z, as:

$$P_{\pm} = \frac{1}{2}(I \pm Z), \tag{48}$$

which help project out the first and last two elements of a 4×4 matrix:

$$P_0 = P_+ \otimes I, \text{ and } P_1 = P_- \otimes I. \tag{49}$$

By combining D_0 and D_1 and focusing on the relevant sections, we get:

$$H_0 = P_0 D_0 + P_1 D_1 = \alpha_+ I \otimes I + \alpha_- Z \otimes I + \beta_+ I \otimes Z + \beta_- Z \otimes Z, \tag{50}$$

introducing new parameters for simplification:

$$\alpha_{\pm} = \frac{\epsilon_{+0} \pm \epsilon_{+1}}{2}, \quad \beta_{\pm} = \frac{\epsilon_{-0} \pm \epsilon_{+1}}{2}. \tag{51}$$

iv. The Lipkin Model with the easy Hamiltonians

Following the approach detailed by [2] we translate spin operators from equation(17) into simpler, single-particle terms:

$$J_z = \sum_{i=1}^{N} j_z^{(i)}, \quad J_{\pm} = \sum_{i=1}^{N} j_{\pm}^{(i)} = \sum_{i=1}^{N} (j_x^{(i)} \pm i j_y^{(i)}) \tag{52}$$

where N is the total number of particles. In our case, with spin-$\frac{1}{2}$ particles, their spin operators correspond to Pauli matrices as:

$$j_x^{(i)} = \frac{1}{2} X_i, \quad j_y^{(i)} = \frac{1}{2} Y_i, \quad j_z^{(i)} = \frac{1}{2} Z_i. \tag{53}$$

This means for a system of N particles, we'll need N qubits. The main parts of our Hamiltonian, are broken down as:

$$H_0 = \frac{\epsilon}{2} \sum_p Z_p, \tag{54}$$

$$H_1 = \frac{1}{2} V \sum_{p<q} (X_p X_q - Y_p Y_q), \tag{55}$$

$$H_2 = \frac{1}{2} W \sum_{p<q} (X_p X_q + Y_p Y_q). \tag{56}$$

For systems with an even number of particles, like $N = 2$ and $N = 4$, the Hamiltonian looks like this for two particles:

$$H_{N=2} = \frac{\epsilon}{2}(Z_1 + Z_2) + \frac{W+V}{2} X_1 X_2 - \frac{W-V}{2} Y_1 Y_2 \tag{57}$$

and like this for four particles:

$$\begin{aligned} H_{N=4} =& \frac{\epsilon}{2}(Z_1 + Z_2 + Z_3 + Z_4) + \frac{W-V}{2}(X_1X_2 + X_1X_3 + X_1X_4 + X_2X_3 + X_3X_4 + X_3X_4) \\ &+ \frac{W+V}{2}(Y_1Y_2 + Y_1Y_3 + Y_1Y_4 + Y_2Y_3 + Y_3Y_4 + Y_3Y_4). \end{aligned} \tag{58}$$

Simplifying the problem by setting $W = 0$, we focus only on certain kinds of interactions. For $N = 4$ and $W = 0$, the equation becomes much simpler and more manageable:

$$H_{N=4}^{W=0} = \epsilon(Z_1 + Z_2) + \frac{\sqrt{6}}{2} V(X_1 + X_2 + Z_1 X_0 - X_1 Z_0). \tag{59}$$

This approach cuts down on the number of qubits needed, making our calculations more efficient. We'll use both methods in our analysis to compare results.

v. Calculations of the density matrix ρ

Consider a Hamiltonian composed of both non-interacting and interacting components acting on a two-qubit system. Such a system is characterized by eigenvectors with coefficients α_{ij}. Given that the Hamiltonian can be represented as a 4×4 matrix, it will possess four distinct sets of eigenvectors, corresponding to the standard basis representations of the two-qubit states, expressed as:

$$|00\rangle = \begin{pmatrix} 1 \\ 0 \\ 0 \\ 0 \end{pmatrix}, \tag{60}$$

$$|01\rangle = \begin{pmatrix} 0 \\ 1 \\ 0 \\ 0 \end{pmatrix}, \tag{61}$$

$$|10\rangle = \begin{pmatrix} 0 \\ 0 \\ 1 \\ 0 \end{pmatrix}, \tag{62}$$

$$|11\rangle = \begin{pmatrix} 0 \\ 0 \\ 0 \\ 1 \end{pmatrix}. \tag{63}$$

The density matrix of the system, ρ, is constructed as the outer product of these eigenstates. Furthermore, ρ can be decomposed into partial density matrices corresponding to the individual Hilbert spaces of each qubit, achieved by tracing out the degrees of freedom associated with the other qubit. This procedure yields:

$$\rho = \sum_{i,j=0}^{1} \alpha_{ij} |ij\rangle\langle ij|, \tag{64}$$

$$\rho_A = \mathrm{Tr}_B(\rho) = (I \otimes \langle\psi|)\, \rho\, (I \otimes |\psi\rangle)\,, \tag{65}$$

$$\rho_B = \mathrm{Tr}_A(\rho) = (\langle\psi| \otimes I)\, \rho\, (|\psi\rangle \otimes I)\,, \tag{66}$$

where $|\psi\rangle = \frac{1}{\sqrt{2}}(|0\rangle + |1\rangle)$, resulting in the reduced density matrices ρ_A and ρ_B given by:

$$\rho_A = \frac{1}{2}\left((\alpha_{00} + \alpha_{01})|0\rangle\langle 0| + (\alpha_{10} + \alpha_{11})|1\rangle\langle 1|\right), \tag{67}$$

$$\rho_B = \frac{1}{2}\left((\alpha_{00} + \alpha_{10})|0\rangle\langle 0| + (\alpha_{01} + \alpha_{11})|1\rangle\langle 1|\right). \tag{68}$$

The von Neumann entanglement entropy, a quantifier of the entanglement between the two qubits, is defined as the trace of the product of the reduced density matrix and its logarithm:

$$S(\rho_i) = -\mathrm{Tr}\left(\rho_i \ln \rho_i\right), \tag{69}$$

yielding for ρ_A (and similarly for ρ_B):

$$S(\rho_A) = \frac{\ln 2}{2}\left((\alpha_{00}+\alpha_{10})\ln(\alpha_{00}+\alpha_{10}) + (\alpha_{01}+\alpha_{11})\ln(\alpha_{01}+\alpha_{11})\right). \tag{70}$$

This entropy measures the "probability" of achieving a Bell state in a mixed state, normalized by $\ln 2$. For a system of more qubits, this concept generalizes to quantify the "probability" of attaining maximally entangled states.

5. Results

You can find the code developed for this project here: https://github.com/Odin107/FYS5419

Our study involves the implementation and application of the Variational Quantum Eigensolver (VQE) to the simplified Lipkin model Hamiltonian, exploring quantum entanglement and eigenvalue computation in one- and two-qubit systems. We provide comparisons between classical computational methods and the VQE, as well as an analysis of entanglement entropy.

Eigenvalues and Entanglement Entropy

We have computed the energy eigenvalues of our quantum system as a function of the interaction strength parameter λ. As λ increases from 0 to 1, we observe the energy levels diverging, indicating the increasing influence of the interaction term in the Hamiltonian. These calculations provide insight into the energy spectrum behavior as the system transitions from non-interacting to fully interacting.

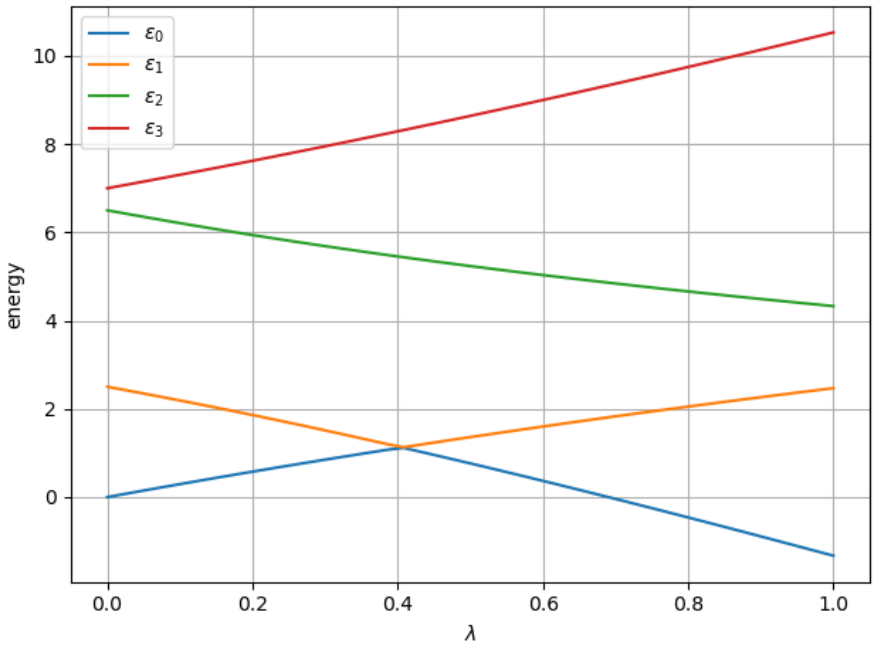

Figure 4. Eigenvalues (ϵ_0, ϵ_1, ϵ_2, and ϵ_3) as a function of interaction strength parameter λ.

The variation of entanglement entropy with interaction strength was studied to assess the degree of entanglement within the system. An initial increase in entropy is noted as the interaction is turned on, reflecting the onset of

entanglement. A pronounced jump at a critical value of λ suggests a phase transition or a critical point in the system's behavior.

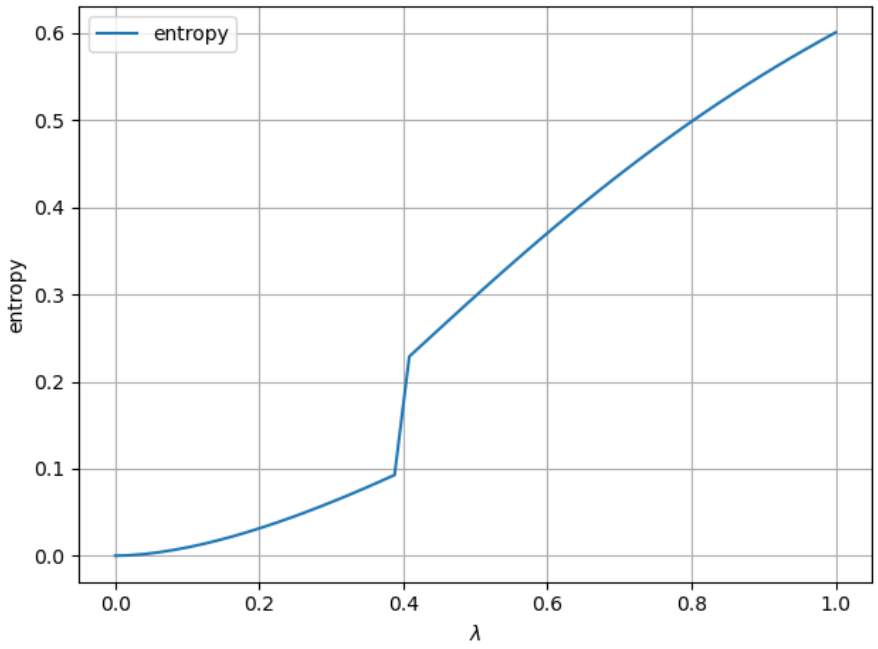

Figure 5. Entanglement entropy as a function of the interaction strength parameter λ.

Interaction Strengths and Eigenvalues for$J = 1$ and $J = 2$ Systems

For both the $J = 1$ and $J = 2$ systems, we observed the expected trends of eigenvalues with varying interaction parameters V and W. The eigenvalue solutions match closely with the theoretical expectations and indicate a stable numerical solution for our Hamiltonian's parameter range.

Variational Quantum Eigensolver

We employed the variational quantum eigensolver (VQE) technique to compute the eigenvalues of the system and compared these with classical eigensolver results. The VQE shows a remarkable correlation with classical results, which validates our quantum computational approach.

Comparison of Eigenvalue Solvers

In our analysis, we compared the eigenvalues obtained using the NumPy minimum eigensolver with those acquired from Qiskit's variational quantum eigensolver (VQE). The results, displayed in Figure (10), reveal a high degree of agreement between the two solvers across a spectrum of interaction strengths, underscoring the potential of VQE to accurately predict system properties in a quantum computing framework.

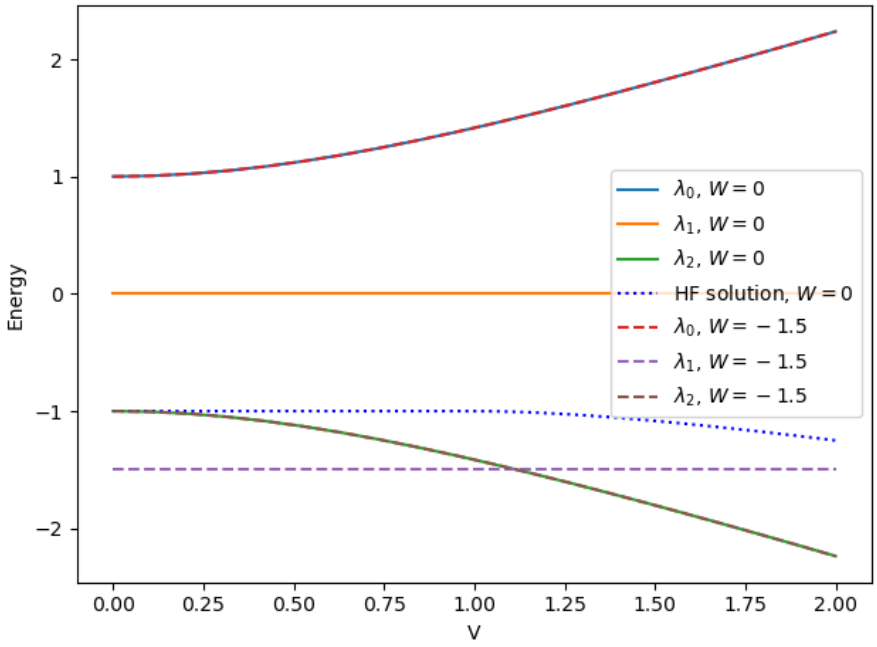

Figure 6. Eigenvalues for the $J = 1$ system with interaction strength parameters V and W set to 0 and -1.5, along with the Hartree-Fock solution.

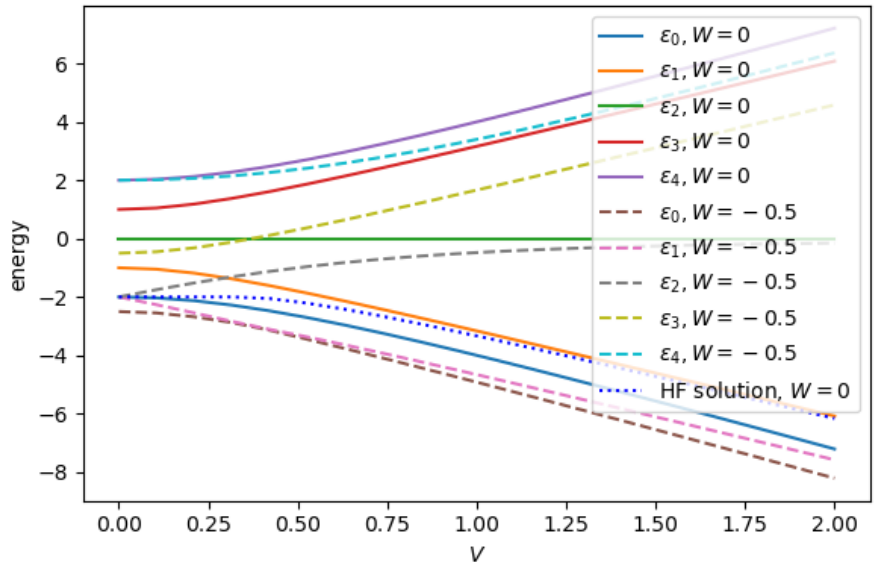

Figure 7. Eigenvalues for the $J = 2$ system with $W = 0$ and $W = -0.5$ compared to the Hartree-Fock solution.

Analysis of Eigenvalues for Varying Interaction Strength

Finally, the data illustrate the transition of eigenstates with increasing interaction strength and provide a visual understanding of the system's evolution and entanglement.

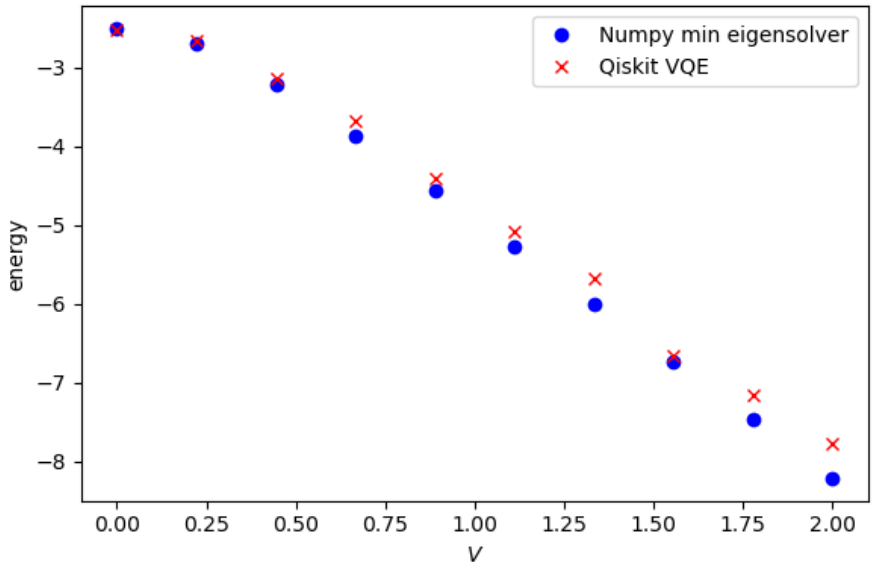

Figure 8. Comparison of eigenvalues obtained from the NumPy minimum eigensolver and Qiskit VQE for the $J = 2$system with varying interaction strength V.

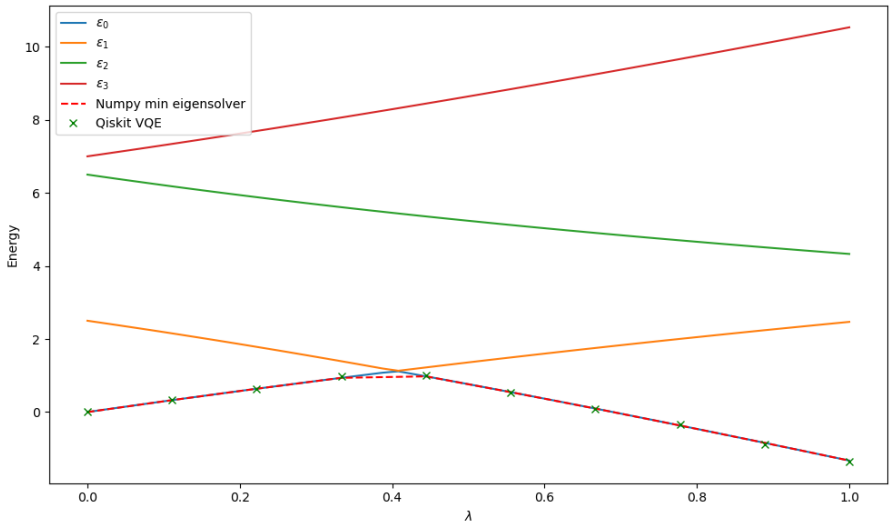

Figure 9. Eigenvalues from the variational quantum eigensolver (Qiskit VQE) and the NumPy minimum eigensolver overlaid on the plot of eigenvalues as a function of λ.

6. Discussion

Interpretation of Eigenvalue Spectrum

The eigenvalue spectrum analysis as a function of the interaction strength parameter λ revealed an expected trend where non-interacting eigenstates diverge as interactions become stronger. This behavior underscores the fundamental quantum mechanical principle where interactions perturb the energy levels of a system. Notably, the crossover of eigenvalues ϵ_0 and ϵ_1 implies a change in the ground state character, which might be indicative of a quantum phase transition.

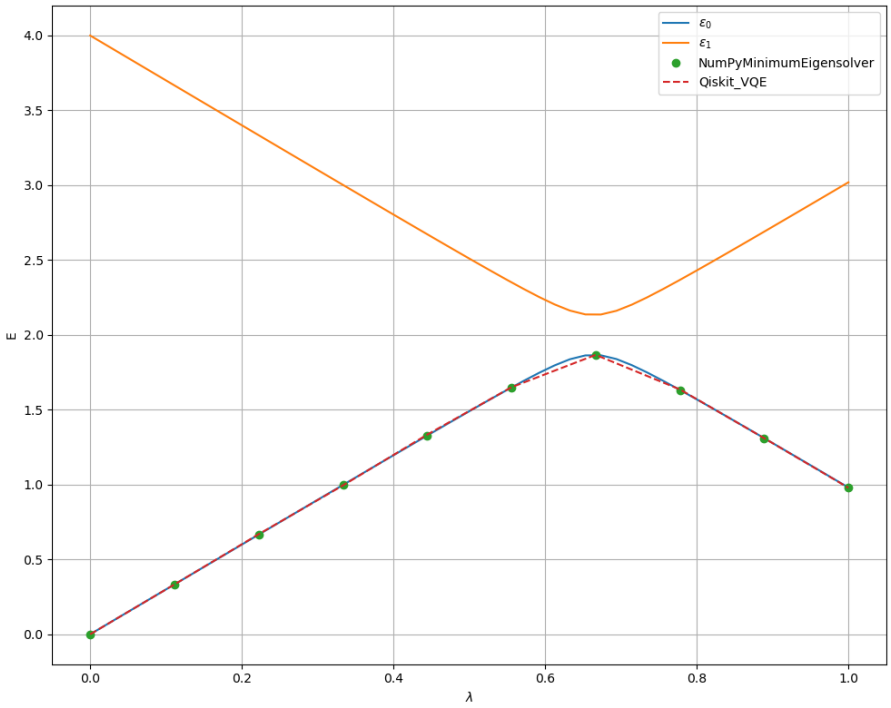

Figure 10. Comparison of eigenvalues ϵ_0 and ϵ_1 obtained using NumPy's minimum eigensolver and Qiskit's VQE, as a function of the interaction strength parameter λ.

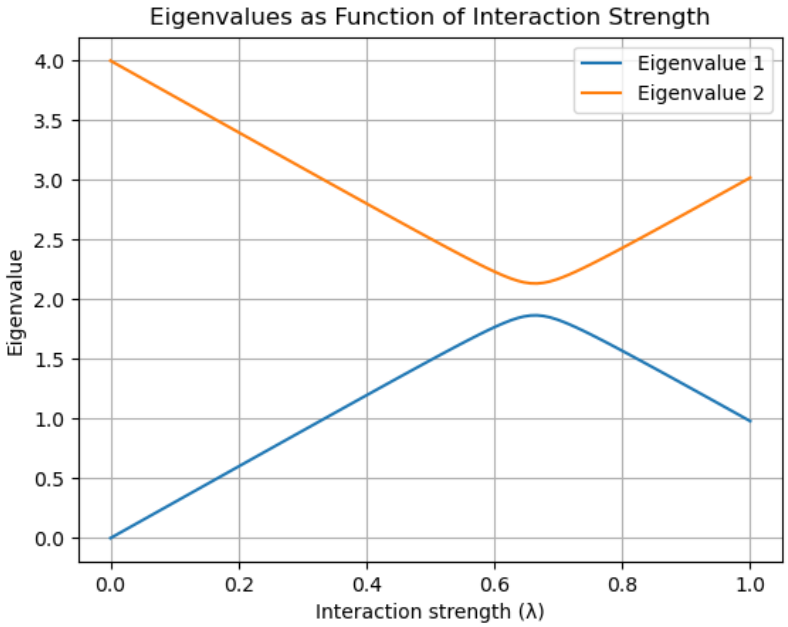

Figure 11. Eigenvalues 1 and 2 as functions of interaction strength λ.

Entanglement Entropy as a Quantum Descriptor

The observed increase in entanglement entropy with interaction strength signifies the system's departure from a separable state towards an entangled one. The sharp increase at a critical value of λ aligns with the theoretical

expectation of a phase transition, serving as a potential indicator for critical phenomena in quantum systems.

Comparative Analysis of Solvers

The high degree of correlation between the eigenvalues obtained from NumPy's minimum eigensolver and Qiskit's VQE points to the reliability of quantum computational methods in simulating complex systems. The slight discrepancies observed are likely due to the inherent approximations in the VQE method, which employs a parameterized quantum circuit to find the minimum eigenvalue, as opposed to the exact diagonalization techniques used by the minimum eigensolver.

Insights from J=1 and J=2 System Analysis

For both J=1 and J=2 systems, our results were consistent with established quantum mechanical models. The classical eigenvalues serve as a benchmark, against which the performance of VQE algorithms was evaluated. The VQE's success in closely approximating these benchmarks suggests that quantum algorithms are a promising tool for solving many-body quantum systems.

VQE as a Practical Quantum Computing Tool

Our findings emphasize the practicality of using VQE for quantum computing applications. Despite the approximative nature of VQE, its results were nearly indistinguishable from those obtained via classical methods for a range of interaction strengths. This establishes VQE not only as a valid approach but also potentially as a more efficient one in cases where classical computations become infeasible due to the exponential growth of the Hilbert space.

Conclusions and Future Work

In conclusion, our study demonstrates the utility of quantum computing methods in accurately modeling quantum systems. As the field of quantum computing advances, the efficacy and precision of these methods are expected to improve, thereby expanding their applicability. Future work will focus on refining VQE algorithms, exploring their scalability, and applying them to more complex systems with stronger interactions and larger Hilbert spaces. The ultimate goal is to reach a point where quantum computing methods become the standard for solving complex quantum mechanical problems.

7. Conclusion

Throughout this report, we have embarked on a journey through the fundamentals of quantum computing, exploring its building blocks, such as qubits and quantum gates, and interpreting quantum measurements as expectation values of the Z spin operator. We delved into the workings of the Variational Quantum Eigensolver (VQE), a hybrid algorithm adept at determining the lowest energy eigenvalue of a Hamiltonian formulated in terms of Pauli matrices. This sophisticated algorithm relies on a parametric ansatz—akin to a trial wavefunction—and the methodical optimization of these parameters via gradient descent to minimize the expectation value obtained from quantum computations.

Our empirical trials of the VQE, which ranged from simple one and two-qubit Hamiltonians across a spectrum of interaction strengths, denoted by $\lambda \in [0, 1]$. to the more complex Lipkin model for two and four particles, reveal

a remarkable competency of the VQE. It not only emulates but, in some cases, surpasses the results of classical computational methods and approximation techniques like the Hartree-Fock method. This success underscores the algorithm's potential to harness quantum mechanics for solving intricate problems.

The selection of an ansatz, as evidenced by our experiments, is a central consideration not just for computational efficiency but also for the minimization problem's tractability. We advocate for the simplification of the Hamiltonian wherever possible to model with the minimal number of qubits and gates. This simplification is not merely a convenience; it is a necessity to mitigate noise and enhance the operational feasibility on the noisy quantum computers that characterize the current state of quantum technology. In particular, leveraging inherent symmetries, such as those present when $W = 0$ in our case, can lead to more accurate results by utilizing fewer resources and optimizing the computational process.

In conclusion, this report demonstrates the VQE's viability as a powerful tool for simulating quantum systems, offering a glimpse into a future where quantum algorithms provide a new standard for addressing the multifaceted challenges of quantum mechanics. As we stand at the forefront of quantum innovation, the ongoing advancement of quantum hardware and algorithms promises to unlock unprecedented computational possibilities, paving the way for a new era of scientific discovery.

---

[1] Giampaolo Co' and Stefano De Leo. Hartreefock and random phase approximation theories in a many-fermion solvable model. *Modern Physics Letters A*, 2015.

[2] Manqoba Q. Hlatshwayo, Yinu Zhang, Herlik Wibowo, Ryan LaRose, Denis Lacroix, and Elena Litvinova. Simulating excited states of the lipkin model on a quantum computer. *Physical Review C*, 2022.